INVERSION OF TOTAL SUSPENDED MATTER CONCENTRATION IN WULIANGSU LAKE BASED ON SWARM INTELLIGENCE OPTIMIZATION AND BP NEURAL NETWORK

Chenhao WU[1], Xueliang FU[2,*], Honghui LI[3], Hua HU[4], Xue LI[5]

Total suspended matter (TSM) is an important parameter of the water environment. Because of the optical complexity in water body, it is difficult to accurately invert the TSM concentration by current traditional methods. In this paper, using Sentinel-2 remote sensing images as the data source combined with measured data, taking Wuliangsu Lake as the study area, a new intelligent algorithm combining the adaptive ant colony exhaustive optimization algorithm (A-ACEO) feature selection method with genetic algorithm (GA) optimized back propagation neural network (BPNN) model (GA-BP) is proposed for inversion of TSM concentration. The ant colony algorithm (ACO) is improved to select remote sensing feature bands for TSM concentration by introducing relevant optimization strategies. The GA-BP model is built by optimizing BPNN using GA with the selected feature bands as input and comparing with the traditional BPNN model. The results show that using feature bands selected by the presented A-ACEO algorithm as inputs, can effectively reduce complexity and improve inversion performance of the model, under the condition of the same model, which can provide valuable references for monitoring the TSM concentration in Wuliangsu Lake.

Keywords: Improved ant colony algorithm, Genetic Algorithm, Back propagation neural network, Wuliangsu Lake, Total suspended matter concentration, Sentinel-2

[1] Master., Dept. of Computer and Information Engineering, Inner Mongolia Agricultural University, China, e-mail: 3206319322@qq.com
[2] Prof., Dept. of Computer and Information Engineering, Inner Mongolia Agricultural University, China,
* Corresponding Author, Inner Mongolia Autonomous Region Key laboratory of Big Data Research and Application of Agriculture and Animal Husbandry, China, e-mail: fuxl@imau.edu.cn
[3] Prof., Dept. of Computer and Information Engineering, Inner Mongolia Agricultural University, China, e-mail: lihh@imau.edu.cn
[4] Master., Dept. of Computer and Information Engineering, Inner Mongolia Agricultural University, China, e-mail: huhua@imau.edu.cn
[5] Master., Dept. of Computer and Information Engineering, Inner Mongolia Agricultural University, China, e-mail: 1441652484@qq.com

1. Introduction

Lake wetland is one of the most important ecosystems in the world [1] and an important safeguard for human social ecological environment [2]. However, with the continuous development, frequent human activities have seriously affected aquatic environment of lake wetlands, and various water resources problems have emerged, causing a serious decline in water quality and affecting regional ecological environment and sustainable economic development [3]. Total suspended matter (TSM) is an essential indicator to evaluate the water quality status of lake wetlands, its concentration not only affects the distribution of the underwater light field, but also affects the primary productivity and the ecological environment of the water area [4]. As an important part of "One Lake, Two Seas" in Inner Mongolia, Wuliangsu Lake has the characteristics of a typical cold and arid lake in the north [5] and belongs to the Hetao Irrigation District, which carries the receding water of agricultural fields for spring irrigation and autumn watering and the discharge of industrial pollution wastewater in the region [6]. Therefore, inversion of TSM concentration in Wuliangsu Lake can estimate lake TSM content, which is of great practical significance for understanding the regional water ecosystem and managing the water environment.

Traditional water quality monitoring are time-consuming, costly and influenced by external conditions [7], which have shortcomings for monitoring large-scale water quality. Remote sensing technology, as one of the important means of environmental monitoring, has become a widely used method to monitor TSM concentration in the environmental monitoring of lake wetlands because of its advantages of rapid, real-time, wide coverage and easy access to data [8]. Previously, many scholars have performed inversion of TSM concentration based on the bands contained within the remote sensing data. For the multiple feature bands present in remote sensing data, they can be broadly classified into single-band, multi-band combination and full-band combination for inversion modeling. When using single-band for modeling, the band data is poorly sensitive to TSM, decreasing model accuracy [9]. When using full-band combination for modeling, the band data may interact with each other, which will also affect the accuracy of TSM concentration inversion [10]. In conclusion, in the study of remote sensing feature bands, determining the characteristic variables of TSM is the first prerequisite to simplify the structure of the inversion model to achieve data compression and increase the efficiency of model operation to reduce computational resources, and many scholars tend to choose the most relevant band combination with TSM concentration [11].

Remote sensing feature selection can be classified into two methods. The first feature selection method is based on mathematical statistics, some

commonly used methods are correlation coefficient analysis (CC), successive projection algorithm (SPA), competitive adaptive reweighted sampling (CARS), etc. For example, Camiolo et al [12] used CC to analyze the data from MODIS-Aqua satellite and TSM concentrations in Río de la Plata, and selected the variables with strong correlation coefficients among them to construct an inversion model with TSM concentration. Luan et al [13] analyzed and selected the feature bands using SPA and CARS, respectively, to finally construct a model of TSM concentration in Yangtze estuary. Although these methods can eliminate the influence of some redundant information to some extent, after feature selection redundant variables are still present, and the stability of the model is poor. The second is based on swarm intelligence optimization algorithm. For example, Jiang et al [14] used GA for analyzing and selecting spectral features and constructed a water quality inversion model of East Lake. Eleyan et al [15] used particle swarm algorithm (PSO) for feature vector selection and successfully reduced the dimension of the features, reduced the complexity of the model. Pamiri et al [16] used ACO for feature selection and achieved high inversion accuracy. These algorithms, which solve optimization problems by group behavior and have a rigorous theoretical basis, provide feasible solutions to complex problems that cannot be handled in traditional methods.

Traditional remote sensing inversion methods can be broadly classified into three methods. The empirical method [17] is relatively simple and possesses good results in linear relationships, but the relationship between remotely sensed spectral features and water body elements is difficult to represent as a simple linear function and the empirical method is usually poorly adaptive. The semi-empirical method [18] and the analytical method [19] are inversion methods that mainly use the optical features inherent in the water column and combine them with remotely sensed reflectance. These methods require more optical data, the models are more complex, and the demand for data hardly be met in practical applications, which is not suitable for wide application. Currently, machine learning as a new method has been widely used in remote sensing inversion. For example, Nazeer et al [20] studied TSM concentration in coastal waters and constructed two machine learning models, which showed that machine learning methods can be more accurate and effective for routine detection of TSM concentration in coastal water. Liu et al [21] analyzed the TSM concentration in Nansi Lake and then constructed linear and machine learning models, which showed that machine learning models have advantages and are more accurate in the inversion of the TSM concentration. Neural network, an important part of machine learning, as it can adapt to more complex nonlinear relationships, has demonstrated strong usability in remote sensing inversion methods. For example, Hafeez et al [22]

performed inversion of TSM concentration in Hong Kong coastal waters by various machine learning methods, in a result, neural networks based on machine learning methods have the better inversion results. Song et al [23] constructed an artificial neural network (ANN) model to invert the TSM concentration caused by the reclamation of an artificial island airport offshore of Bohai Sea, China, and obtained good results. In general, the traditional remote sensing inversion method is simple, but it is not widely used due to its characteristics, while machine learning as a new method has been more widely used in remote sensing inversion methods, and neural network also has strong applicability in remote sensing inversion methods because of its advantages.

In conclusion, taking Wuliangsu Lake as the study area, the correlation between remote sensing features and TSM is analyzed by combining Sentinel-2 remote sensing images and measured data. Through the analysis, a swarm intelligence optimization algorithm is proposed as an adaptive ant colony exhaustive optimization (A-ACEO) algorithm which is used for remote sensing feature bands selection. Taking the selected feature bands as inputs and considering the advantages of swarm intelligence optimization algorithm and neural network, the GA-BP model was constructed by using GA to optimize the BPNN. Finally, through the study, the model is analyzed and verified the performance of the method.

2. Feature Band Selection Methods and Modelling

2.1 Feature Band Selection Method

2.1.1 Competitive Adaptive Reweighted Sampling Algorithm

The competitive adaptive reweighted sampling (CARS) algorithm is based on Darwinian evolutionary theory of "survival of the fittest" [24], treating each feature as an individual and selecting individuals with high adaptive capacity. The specific steps are shown below:

(1) Randomly selected N samples in the feature band using Monte Carlo algorithm and constructed partial least squares regression (PLSR) model.

(2) The variables are selected by exponentially decreasing function (EDF) and adaptive reweighted sampling algorithm (ARS), where high regression coefficients are retained, and low ones are removed.

(3) A new subset is set to hold the reserved variables and the PLSR model is constructed, meanwhile the root mean square error of cross validation (RMSECV) is calculated.

(4) Repeat Step (1)-(3), after N calculations, N samples will obtain N subsets of variables, and N subsets of variables will obtain N RMSECVs. End up selecting the smallest subset as the optimal feature band combination.

2.1.2 Standard Ant Colony Optimization Algorithm

The ant colony (ACO) algorithm is a swarm intelligence optimization algorithm that simulates the foraging behavior of ants [25]. ACO algorithm was originally designed to solve static combinatorial problems, but it also has good applicability in dynamic combinatorial optimization problems [26]. Therefore, ACO algorithm presents feasibility in the feature band selection method.

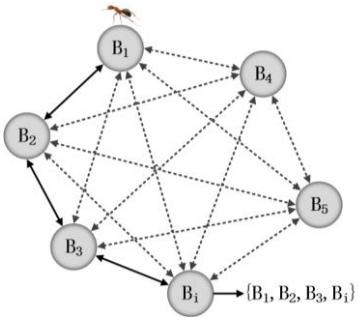

Fig. 1. Visualization of ACO algorithm to select feature bands

As shown in Fig. 1, each node in the figure corresponds to a feature band, where {B_1, B_2, …, B_i} is the set of original feature bands. An ant randomly starts from a node and selects another node according to the rules, after a period of traversal, a subset of original feature bands {B_1, B_2, B_3, B_i} will be obtained, and if this subset satisfies the stopping condition, it is judged to be a feasible solution. The ACO algorithm is shown below:

(1) Initialization of the pheromone concentration. The initial pheromone of all nodes is set to 1, and the initial nodes are randomly selected according to the roulette method.

(2) Node selection probability. The next node is selected by the ant through the pheromone concentration presented at the node, and the probability from node B_i to node B_j is shown in equation (1):

$$P_{ij}(t)=\begin{cases}\dfrac{\tau_{ij}(t)}{\sum_{J}\tau_{ij}(t)}, & j\in J\\ 0, & \text{Other}\end{cases} \tag{1}$$

where, t is the iteration number, τ is the node pheromone concentration, and J is the collection of unselected nodes reachable by ants at node B_i.

(3) Feature subset objective function selection. The feature subset function F is calculated based on the root mean square error (RMSE), as shown in equation (2):

$$F=\frac{C}{1+RMSE} \tag{2}$$

where C is a constant term that is usually set to 1. The equation shows that the smaller the RMSE, the easier the subset is selected.

(4) Pheromone concentrations updating. Once all ants have completed one iteration, the node pheromone concentration will be updated, the node pheromone concentration within the selected subset set increases, and the remaining node pheromone concentration volatilizes, as shown in equations (3)-(4):

$$\tau_{ij}(t+1) = (1-\rho)\,\tau_{ij}(t) + \triangle\tau_{ij}(t) \tag{3}$$

$$\triangle\tau_{ij}(t) = \begin{cases} F, <i, j> \in B \\ 0, Other \end{cases} \tag{4}$$

where ρ is the pheromone volatility factor between (0,1), B is the set of selected subsets of feature bands.

2.1.3 Adaptive Ant Colony Exhaustive Optimization Algorithm

Although standard ACO algorithm has good advantages in solving dynamic combinatorial problems, the initial parameters tend to influence the algorithm, which can easily lead to too slow convergence and relatively low efficiency [27]. The adaptive ant colony exhaustive optimization (A-ACEO) algorithm improves the corresponding strategy based on the standard ACO algorithm, so that it can accelerate the convergence speed and improve efficiency. And the combination of ACO algorithm and exhaustive method [28] is used to effectively prevent the algorithm dropping into local optimum, meanwhile avoiding exhaustive search of the subset of bands by the exhaustive method, which greatly reduces the search time. The A-ACEO algorithm process is as follows:

(1) Adaptive adjustment strategy of initialized pheromone concentration. The initial pheromone concentration coefficients of the nodes are mostly the same and fixed values in standard ACO algorithm, and the ants will randomly select a node as the initial node, which makes the algorithm converge slowly and inefficiently. To solve the above problem, the reciprocal of RMSE corresponding to each node is used as the initial pheromone concentration based on GA-BP model to guide ants in selecting the initial nodes, which avoids the shortage of the ants finding nodes randomly in the iterations.

(2) Adaptive adjustment strategy of volatilization factor ρ. In ACO algorithm, the volatility factor is a fixed value, if the value is not set reasonably will affect the convergence speed, or even lose the full search ability. To solve the above problem, ρ is made adaptive adjustment strategy to enhance the algorithm search capability, as shown in equation (5):

$$\rho(t+1) = \frac{T}{t+T} e^{1-\rho(t)} \tag{5}$$

where t and T are the current and maximum iteration number respectively. It is clear that initially, ρ has a larger value, with more and more iterations, ρ decreases, the probability of the optimal node gradually increases.

(3) Adaptive updating strategy of pheromone concentration. The pheromone concentration update strategy is improved with standard ACO algorithm as shown in equations (6)-(7):

$$\tau_{ij}(t+1)=(1-\rho)\tau_{ij}(t)+\Delta\tau_{ij}(t) \tag{6}$$

$$\Delta\tau_{ij}(t)=\begin{cases}\lambda_{ij}+Q\times\dfrac{1}{R_{ij}(t)}, <i,j>\in B\\ 0, \qquad\qquad Other\end{cases} \tag{7}$$

Where λ_{ij} is the initialized pheromone concentration of the node selected by the ant, Q is the pheromone heuristic factor, B is the set of the selected subset of feature bands, $R_{ij}(t)$ is the RMSE of the selected subset of nodes at the t-th iteration.

(4) Optimal threshold and optimal matrix strategy. Combining the standard ACO algorithm with the exhaustive enumeration method, an optimal threshold and optimal matrix strategy is proposed, which uses the optimal threshold to filter the subset of nodes generated by the iterations and deposits the subset of nodes larger than the optimal threshold into the optimal matrix. At last, the optimal node subset is selected from the optimal matrix, which is the optimal feature subset. By filtering, this strategy significantly reduces the space of data storage and the consumption of computational resources. The optimal threshold is shown in equation (8):

$$O(t)=\frac{1}{R_{xy}(t)}, <x,y>\in B_m \tag{8}$$

where B_m is the pheromone concentration set of nodes in order from highest to lowest, R_{xy} is the RMSE of the set of subsets of nodes with the highest pheromone concentration.

2.2 Inversion Method for TSM Concentration

In order to avoid the model falling into local optimum and to improve the accuracy of model inversion. This paper proposes a GA-BP inversion model by optimizing the BPNN with the global search capability of GA, based on BPNN.

2.2.1 Back propagation Neural Network

Back propagation neural network (BPNN) is a multilayer feedforward network with forward transmission of signals and backward propagation of errors [29]. The BPNN topology is shown in Fig. 2. In forward transmission, the signal will be transmitted sequentially from input layer to hidden layer and then to output layer, and the signal will be processed according to a certain function mapping relationship between layers, and finally the output will be output at output layer, and if the output is not within the expectation, the error will be back propagated. In back propagation, the error is propagated in reverse order, from output layer, and

the gradient descent method is used to adjust the weights and thresholds of the nodes in each layer, and subsequently, the next step of forward propagation is started again, and the error is continuously adjusted to the minimum.

2.2.2 Genetic Algorithm to Optimize BPNN

Although BPNN has been applied in many fields, it is easy to fall into local optimum and has poor inversion effect.

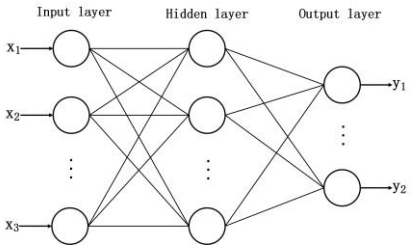

Fig. 2. BP neural network topology

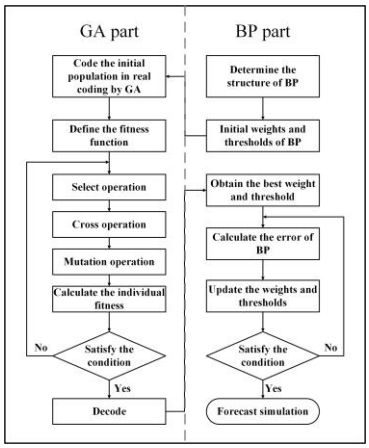

Fig. 3. Flow chart of the GA-BP model

The GA-BP model process is as follows:

The genetic algorithm (GA) is a stochastic search method that simulates natural selection in nature [30]. GA is a gradient-free optimization and search technique that can randomly generate starting points from different directions and perform adaptive search in the solution space by the guidance of fitness function. Therefore, the global search capability of GA is used to optimize BPNN, which can improve the shortcomings of BPNN and accelerate the learning speed of BPNN at the same time. The process of GA-BP model is shown in Fig. 3.

(1) Determination of network topology. The A-ACEO algorithm is used to select feature bands as input layers and TSM concentrations as output layers.

(2) Initialization of population. The weights and thresholds in the network are initialized and then encoded as a set of chromosomes. The population size is set to M.

(3) Definition of fitness function. The sum of the absolute errors of the measured and inverse suspended matter concentrations from GA-BP model is taken as the inverse of the fitness function F. The larger the F, the higher the fitness. As shown in equation (9):

$$F = \frac{1}{\sum_{i=1}^{n} (y_i - \hat{y}_i)^2} \tag{9}$$

where y_i and $\hat{y}_i$ are the measured and inverse values of TSM concentration.

(4) Select operation. The probability is determined using the roulette selection method and the best individual is selected to enter the next generation.

(5) Cross operation. Individuals are randomly selected for exchange and combination operations to produce more adaptable individuals.

(6) Mutation operation. An individual is randomly selected in the population, and a portion of its genes in which are selected to exchange and vary with their alleles, so as to produce individuals with stronger fitness.

(7) Calculating individual fitness. Determine if the stop condition is satisfying, if so, Step8 is executed; otherwise, Step (4) is executed.

(8) Decoding. The weights and thresholds of GA output are adapted to BPNN, and the errors are calculated. Once the conditions are met, the final inversion results are output.

In conclusion, the inversion of TSM concentration in Wuliangsu Lake based on Swarm Intelligence Optimization and BPNN is shown in Fig. 4.

3. Simulation Experiment

3.1 Study Area

Wuliangsu Lake (40°36′N-41°03′N, 108°43′E-108°57′E), as shown in Fig. 5, located in Bayan Nur City, Inner Mongolia, is the biggest lake wetland at the same latitude in the world. The lake covers an area of 325.31km$_2$, in which 123.11km$_2$ is open water and the remaining is reed area, with a reservoir capacity of about 2.5 to 3×10^8m$_3$. The wetland of Wuliangsu Lake is relatively rich in species, inhabited by a large number of fish and birds. However, due to the continuous exploitation of WuliangSu Lake, the lake is decreasing in size, while the wastewater discharged into the lake is increasing year by year and a large number of fish are dying, resulting in serious ecological damage of the lake and gradual degradation of ecosystem function.

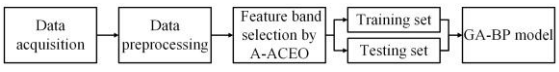

Fig. 4. Overall process of TSM concentration inversion

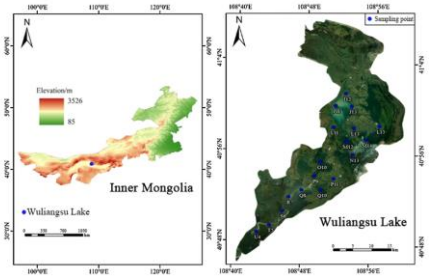

Fig. 5. Location and sampling point distribution of study area

3.2 Measured Data Acquisition

The measured data is provided by the national research team of Inner Mongolia Agricultural University, "River and Lake Wetland Water Environmental

Protection and Restoration Technology Research and Innovation Talent Team", which is dedicated to the research of lake wetlands in the northern cold and arid region for a long time, providing comprehensive big data management and sharing services for ecological protection in China. Wuliangsu Lake starts to freeze in early November every year, and the freezing and thawing period can be up to 5 months, so the sampling time is mainly concentrated in June to September, and the sampling is fixed to the middle and end of each month, and the sampling depth is 0.5m down from the water surface vertically. The measured data of TSM concentration were collected from 2015 to 2018 with 92 groups, some measured data are shown in Table 1, and the training and test sets were randomly divided into 64 and 28 groups.

Table 1.

Selected measured data from 2015-2018

Date of actual test	Remote Sensing Image Dates	Sampling point	Measured TSM concentration (μg/L)
2015/9/25	2015/9/25	I12	22.0
2016/6/20	2016/6/21	S6	26.0
2017/6/25	2017/6/26	J11	1.0
2017/8/29	2017/8/30	L13	41.0
2017/9/25	2017/9/24	J13	197.0
2018/7/26	2018/7/26	M14	2.0

3.3 Remote Sensing Data Acquisition

Developed by the European Space Agency (ESA), the Sentinel-2 satellite can be used to monitor remote sensing images of terrestrial ecology, inland rivers and coastal areas. It is equipped with a multispectral imager (MSI) with 13 spectral bands and three spatial resolutions of 10m, 20m and 60m. Specific satellite data are shown in Table 2. The image data are available on the ESA website (https://scihub.copernicus.eu/dhus/#/home).

Download the quasi-synchronous Sentinel-2L1C class remote sensing image data synchronized with or one day different from the measured data through the European Space Agency (ESA), and set the filtering condition of cloudiness less than 20% before downloading to guarantee clear remote sensing images of Wuliangsu Lake. Remote sensing images are taken at as wide an interval as possible to ensure that the experimental results are more representative. The pre-processing of Sentinel-2 remote sensing image data includes cropping, resampling, geometric correction and band reflectance extraction to obtain remote sensing reflectance in each band. For atmospheric correction of the data, the Sentinel-2L2A level image data was acquired using Sen2Cor plug-in from ESA. When the data was resampled, the S2 Resampling Processor in SNAP software is used, and the resolution is set to 20m using the nearest-neighbour method.

Table 2.

Sentinel-2 sensor spectral characteristic information

Band Number	Sentinel-2A		Sentinel-2B		Spatial resolution(m)
	Central wavelength (nm)	Bandwidth (nm)	Central wavelength (nm)	Bandwidth (nm)	
1	433.9	27	442.3	45	60
2	496.6	98	492.1	98	10
3	560.0	45	559.0	46	10
4	664.5	38	665.0	39	10
5	703.9	19	703.8	20	20
6	740.2	18	739.1	18	20
7	782.5	28	779.7	28	20
8	835.1	145	833.0	133	10
8A	864.8	33	864.0	32	20
9	945.0	26	943.2	27	60
10	1373.5	75	1376.9	76	60
11	1613.7	143	1610.4	141	20
12	2202.4	242	2185.7	238	20

3.4 Model Parameter Setting

Whether A-ACEO or standard ACO algorithms is taken for feature band selection, the setting of parameters needs to be considered. The parameters set need to ensure both stability and efficiency of the algorithm. Table 3 shows the relevant parameter settings for A-ACO-E and ACO algorithms.

Table 3.

The relevant parameter settings for A-ACEO algorithm and ACO algorithm

Parameter	ACO	A-ACEO
Maximum iterations number t	50	50
Initial population size m	20	20
Pheromone volatility factor □	0.1	/
Pheromone inspiration factor Q	5	5

When constructing the GA-BP model, the iteration number is 50, the number of input layers is the number of feature bands obtained by the feature band selection algorithm, the number of hidden layers is half of the number of input layers, the number of output layers is 1. The parameters of GA are set to ensure both stability and accuracy of the model and are shown in Table 4.

Table 4.

GA parameter settings

Parameter	Value (Probability)
Initial population size	300
Maximum iterations number	50
Selection probability	0.02
Crossover probability	0.02
Mutation probability	0.02

3.5 Model Evaluation Metrics

In this paper, the coefficient of determination (R^2) and the root mean square error (RMSE) are used as the evaluation indexes of the inversion model of TSM concentration. The details are shown in equations (10)-(11):

$$R^2 = 1 - \frac{\sum_{i=1}^{n}\left(y_i - \hat{y}_i\right)^2}{\sum_{i=1}^{n}\left(y_i - \bar{y}_i\right)^2} \tag{10}$$

$$RMSE = \sqrt{\frac{1}{n}\sum_{i=1}^{n}\left(y_i - \hat{y}_i\right)^2} \tag{11}$$

where y_i is the measured value of TSM concentration, $\hat{y}_i$ is the inverse value of TSM concentration, $\bar{y}_i$ is the average value of TSM concentration. The closer the R^2 is to 1, the more stable the model is; the smaller the RMSE, the more accurate the model is.

3.6 Results and Analysis

3.6.1 Feature Band Selection

To verify the effect on selecting feature bands for A-ACEO algorithm, the results are compared with CARS algorithm and ACO algorithm, respectively. Fig. 6 shows the optimal RMSE variation curves of the GA-BP model with three bands selection methods. From Fig. 6, we can see that CARS algorithm starts with fast convergence, but it is likely to drop into local optimum and hard to jump out, and the convergence effect is poor. As a swarm intelligence algorithm, the ACO algorithm can avoid the problems of CARS, but when the combinatorial problem is complex, the ACO algorithm may lead to information loss and general convergence effect, making it difficult to find the optimal solution. A-ACEO algorithm not only retains the advantages of ACO algorithm, but also improves the problem of information loss, increases the diversity of feature bands, and achieves a better convergence effect.

To further validate the performance of the A-ACEO algorithm, different feature band selection algorithms are run randomly once. The results are visualized in Fig.7, CARS algorithm selected nine feature bands related to the TSM concentration, and ACO and A-ACEO algorithms selected eight feature bands related to the TSM concentration. Therefore, A-ACEO algorithm not only selects effective feature bands information, but also reduces the influence of redundant feature bands, thus simplifying the model.

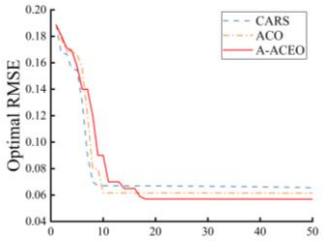

Fig. 6. Optimal RMSE change curve in each iteration

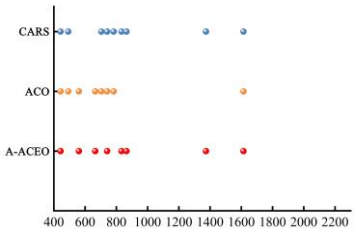

Fig. 7. Visualization of different algorithms to select the feature band

3.6.2 A-ACEO-GA-BP Model Performance and Analysis

In this paper, the GA-BP inversion model is constructed using the feature band selected by full-band, CARS, ACO and A-ACEO algorithms and the measured TSM concentration as the input and output of the model, respectively. Figure 8 presents the inversion results, where the diagonal line in the figure is the 1:1 line between inversion and measured values, and the inversion evaluation metrics are shown in Table 5.

The GA-BP models constructed by four different feature band selection algorithms as input all have good inversion effects. From Fig. 8, most of the values are well-distributed along the 1:1 line, and only a few values are more discrete.

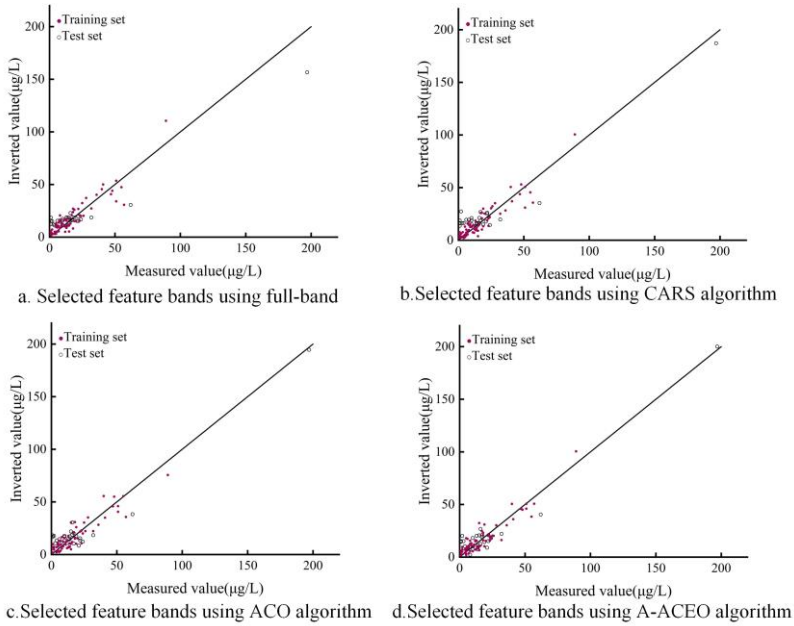

a. Selected feature bands using full-band
b.Selected feature bands using CARS algorithm
c.Selected feature bands using ACO algorithm
d.Selected feature bands using A-ACEO algorithm

Fig. 8. Inversion results of the GA-BP models for different feature band selection algorithms

From Table 5, the results using A-ACEO algorithm combined with GA-BP model is the best, with R^2-C and R^2-P of 0.9074 and 0.9030, respectively, and

RMSE-C and RMSE-P of 0.0568μg/L and 0.0570μg/L, respectively, which are better than the GA-BP model built from feature bands selected by the full-band, CARS and ACO algorithms. Therefore, under the same inversion model, using A-ACEO algorithm for feature band selection can effectively reduce the computational consumption and improve the model inversion performance.

Table 5.

Inversion evaluation metrics of GA-BP models with different feature band selection algorithms

Model	Number of feature bands	Training set		Test set	
		R^2-C	RMSE-C(μg/L)	R^2-P	RMSE-P(μg/L)
GA-BP	12	0.8531	0.0701	0.8424	0.0727
CARS-GA-BP	9	0.8732	0.0652	0.8658	0.0671
ACO-GA-BP	8	0.8880	0.00613	0.8875	0.0614
A-ACEO-GA-BP	8	0.9074	0.0568	0.9030	0.0570

3.6.3 BPNN Model Building and Analysis

The traditional BPNN model is built and compared with the GA-BP model. Fig. 9 presents the inversion results of BPNN model with different feature bands selection algorithms, and the inversion evaluation metrics are shown in Table 6.

From Fig. 9, the inversion accuracy of BPNN model constructed with different feature band selection algorithms is not satisfactory. The inversion effect of the BPNN based on the full-band is the worst compared with CARS, ACO and A-ACEO algorithms. The inversion results of the BPNN model are generally distributed along 1:1 line, and there are some deviations.

From Table 6, compared with the GA-BP models, all BP neural network models have a reduced inversion effect. The inversion accuracy of BPNN model constructed using full-band is the lowest, while the best accuracy is achieved using the A-ACEO algorithm, with R^2-C and R^2-P are 0.7324 and 0.7253, respectively, and RMSE-C and RMSE-P are 0.0923μg/L and 0.0959μg/L, respectively. This further demonstrates that the A-ACEO algorithm has greater advantages and application potential in the selection of feature bands.

In conclusion, GA-BP model outperformed BPNN model in all inversions. It may be due to the fact that updating the weights and thresholds is mainly achieved by using the error function for monotonic ascending or monotonic descending in BPNN, while the inversion of the TSM concentrations in Wuliangsu Lake is a non-linear problem with multiple extremes, and BPNN model will stop adjusting the weights and thresholds when it encounters a local optimum, whereas the GA algorithm has powerful global search capability, which allows individuals in the population do not move in a homogenous direction. Therefore, in this paper, BPNN

is optimized using GA algorithm, which can well invert the TSM concentration in Wuliangsu Lake.

Table 6.

Inversion evaluation metrics of BP models with different feature band selection algorithms

Model	Number of feature bands	Training set		Test set	
		R^2-C	RMSE-C(μg/L)	R^2-P	RMSE-P(μg/L)
BP	12	0.6123	0.1132	0.5963	0.1163
CARS-BP	11	0.6472	0.1083	0.6326	0.1110
ACO-BP	9	0.7071	0.1008	0.6921	0.1016
A-ACEO-BP	8	0.7324	0.0923	0.7253	0.0959

3.7 Spatial and Temporal Distribution of TSM Concentration

Through analyzing different feature bands selection algorithms and different modeling methods, the GA-BP model established with A-ACEO algorithm has the best inversion effect. Therefore, the TSM concentration distribution obtained based on this model is shown in Fig. 10. There are some differences exists in the concentration and spatial distribution of TSM in Wuliangsu Lake with time, which may be related to the fact that Wuliangsu Lake is an extremely important part of the irrigation and drainage system of the Inner Mongolia Loop Irrigation District. Whenever spring irrigation and autumn watering are in progress, a large amount of receding water from agricultural fields will flow into the northern area of Wuliangsu Lake through the drainage and irrigation canals, and then, after purification by the lake, flow out from the receding canals in the southern part of Wuliangsu Lake.

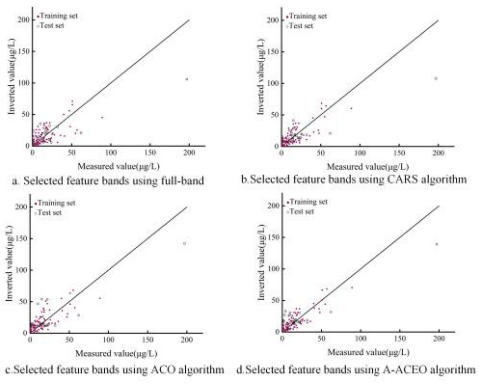

Fig. 9. Inversion results of the BP models for different feature band selection algorithms

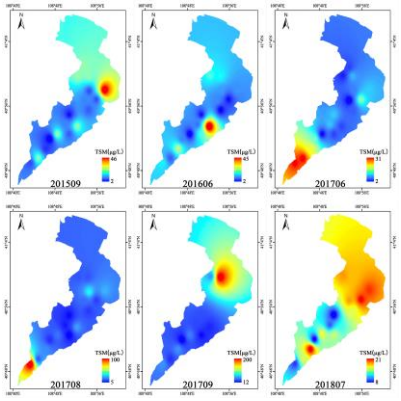

Fig. 10. Distribution of TSM concentration

4. Conclusion

In this paper, using the advantages of swarm intelligence optimization algorithm and neural network, an A-ACEO feature band selection algorithm is

proposed, and GA-BP model is constructed to invert the TSM concentration, which draws the following conclusions:

1. When the inversion model is the same, compared with full-band, CARS algorithm and standard ACO algorithm, A-ACEO algorithm selects fewer feature bands, effectively reducing computational resources and model complexity, while improving the inversion effect of the model.

2. When the feature band selection method is the same, compared with the traditional BPNN model, the GA-BP model has improved the R^2 and RMSE and has better results.The GA-BP model can better invert TSM concentration in Wuliangsu Lake. Among them, the inversion of the GA-BP model based on A-ACEO algorithm is optimal.

Therefore, the proposed method can provide new ideas for the detection of TSM concentration in Wuliangsu Lake, which is helpful to manage the regional water environment system and ecological balance.

Acknowledgements

This research was supported by the National Natural Science Foundation of China (62041211, 61962047), the National Key Research and Development Program of China(2019YFC049205), the Natural Science Foundation of Inner Mongolia Autonomous Region of China (2020MS06011, 2019MS06015, 2021MS06009), the Basic Research Operation Funds for Universities under Inner Mongolia Autonomous Region (BR22-14-05), the Research Program of Science and Technology at Universities of Inner Mongolia Autonomous Region (NJZZ23044), and the Program for Innovative Research Team in Universities of Inner Mongolia Autonomous Region (NMGIRT2313).

REFERENCES

[1]. *Y. Li, Z. Y. Hou, L. Q. Zhang, C. Q. Song, S. L. Piao, J. T. Lin, S. S. Peng, K. Y. Fang, J. Yang, Y. Qu, Y. B. Wang, J. W. Li, R. J. Li, and X. Yao*, "Rapid expansion of wetlands on the Central Tibetan Plateau by global warming and El Niño", Science Bulletin, vol. 68, no. 5, Sept. 2023, pp. 485-488

[2]. *C. Q. Song, L. H. Ke, H. Pan, S. G. Zhan, K. Liu, and R. H. Ma*, "Long-term surface water changes and driving cause in Xiong'an, China: from dense Landsat time series images and synthetic analysis", Science Bulletin, vol. 63, no. 11, Sept. 2018, pp. 708-716

[3]. *Y. Pan, M. Rosenkranz, L. Costadone, and M. D. Sytsma*, "Effect of management on water quality and perception of ecosystem services provided by an urban lake", Lake and Reservoir Management, vol. 37, no. 4, Sept. 2021, pp. 418-430

[4]. *J. Zhao, W. X. Cao, Z. T. Xu, H. B. Ye, Y. Z. Yang, G. F. Wang, W. Zhou, and Z. H. Sun*, "Estimation of suspended particulate matter in turbid coastal waters: application to hyperspectral satellite imagery", Opt. Express, vol. 26, Sept. 2018, pp. 10476-10493

[5]. *Z. Li, Q. Wang, M. Tang, P. Lu, G. Li, M. Leppäranta, J. Huotari, L. Arvola, and L. Shi*, "Diurnal Cycle Model of Lake Ice Surface Albedo: A Case Study of Wuliangsuhai Lake", Remote Sensing, 2021

[6]. *B. B. Shen, J. L. Wu, and Z. H. Zhao*, "A ~150-Year Record of Human Impact in the Lake Wuliangsu (China) Watershed: Evidence from Polycyclic Aromatic Hydrocarbon and Organochlorine Pesticide Distributions in Sediments", Journal of Limnology, 2016

[7]. *Y. M. Zheng, Z. G. Niu, P. Gong, and J. Wang*, "A database of global wetland validation samples for wetland mapping", Science Bulletin, vol. 60, no. 4, Sept. 2015, pp. 428-434

[8]. *Y. Liang, F. Yin, D. Xie, L. Liu, Y. Zhang, and T. Ashraf*, "Inversion and Monitoring of the TP Concentration in Taihu Lake Using the Landsat-8 and Sentinel-2 Images", Remote Sens, 2022

[9]. *P. Duan, F. Zhang, C. Liu, M. L. Tan, J. Shi, W. Wang, Y. Cai, H. T. Kung, and S. Yang*, "High-Resolution Planetscope Imagery and Machine Learning for Estimating Suspended Particulate Matter in the Ebinur Lake, Xinjiang, China", IEEE Journal of Selected Topics in Applied Earth Observations and Remote Sensing, vol. 16, Sept. 2023, pp. 1019-1032

[10]. *Y. Cao, Y. T. Ye, H. L. Zhao, Y. Z. Jiang, H. Wang, Y. Z. Shang, and J. F. Wang*, "Remote sensing of water quality based on HJ-1A HSI imagery with modified discrete binary particle swarm optimization-partial least squares (MDBPSO-PLS) in inland waters: A case in Weishan Lake", Ecological Informatics, vol. 44, Step. 2018, pp. 21-32

[11]. *Q. Guo, H. Wu, H. Jin, G. Yang, and X. Wu*, "Remote Sensing Inversion of Suspended Matter Concentration Using a Neural Network Model Optimized by the Partial Least Squares and Particle Swarm Optimization Algorithms", Sustainability, 2022

[12]. *M. D. Camiolo, E. Cozzolino, A. I. Dogliotti, C. G. Simionato, and C. A. Lasta*, "An empirical remote sensing algorithm for retrieving total suspended matter in a large estuarine region", scimar [Internet], vol. 83, no. 1, Sept. 2019, pp. 53-60

[13]. *K. Luan, H. Li, J. Wang, C. Gao, Y. Pan, W. Zhu, H. Xu, Z. Qiu, and C. Qiu*, "Quantitative Inversion Method of Surface Suspended Sand Concentration in Yangtze Estuary Based on Selected Hyperspectral Remote Sensing Bands", Sustainability, 2022

[14]. *Q. H. Jiang, M. X. Liu, J. Wang, and F. Liu*, "Feasibility of using visible and near-infrared reflectance spectroscopy to monitor heavy metal contaminants in urban lake sediment", CATENA, vol. 162, Sept. 2018, pp. 72-79

[15]. *A. ELEYAN*, "Particle Swarm Optimization Based Feature Selection for Face Recognition", in 2019 Seventh International Conference on Digital Information Processing and Communications (ICDIPC). IEEE, Sept. 2019, pp. 1-4

[16]. *M. Paniri, M. B. Dowlatshahi, and H. Nezamabadi-pour*, "Ant-TD: Ant colony optimization plus temporal difference reinforcement learning for multi-label feature selection", Swarm and Evolutionary Computation, 2021

[17]. *J. Mi, G. Li, D. Ding, L. L. Qiao, Y. Y. Ma, G. Yang, Y. Q. Zhang, L. Zhang, and S. H. Li*, "Temporal-Spatial Variation of Surface Suspended Matter and Controlling Factors in the Inner Shelf of the East China Sea in Winter", Ocean Univ. China, vol. 18, Sept. 2019, pp. 9-19

[18]. *M. Arora, A. Mudaliar, and B. Pateriya*, "Assessment and Monitoring of Optically Active Water Quality Parameters on Wetland Ecosystems Based on Remote Sensing Approach: A Case Study on Harike and Keshopur Wetland over Punjab Region", India. Eng. Proc, 2022

[19]. *F. F. Wang, W. X. Huai, and Y. K. Guo*, "Analytical model for the suspended sediment concentration in the ice-covered alluvial channels", Journal of Hydrology, 2021

[20]. *M. Nazeer, M. Bilal, M. M. M. Alsahli, M. I. Shahzad, and A. Waqas*, "Evaluation of Empirical and Machine Learning Algorithms for Estimation of Coastal Water Quality Parameters", ISPRS Int. J. Geo-Inf, 2017

[21]. *X. Y. Liu, Z. Zhang, T. Jiang, X. H. Li, and Y. Y. Li*, "Evaluation of the Effectiveness of Multiple Machine Learning Methods in Remote Sensing Quantitative Retrieval of Suspended Matter Concentrations: A Case Study of Nansi Lake in North China", Journal of Spectroscopy, 2021

[22]. *S. Hafeez, M. S. Wong, H. C. Ho, M. Nazeer, J. Nichol, S. Abbas, D. Tang, K. H. Lee, and L. Pun*, "Comparison of Machine Learning Algorithms for Retrieval of Water Quality Indicators in Case-II Waters: A Case Study of Hong Kong", Remote Sens, 2019

[23]. *N. Q. Song, N. Wang, W. N. Lin, and N. WU*, "Using satellite remote sensing and numerical modelling for the monitoring of suspended particulate matter concentration during reclamation construction at Dalian offshore airport in China", European Journal of Remote Sensing, vol. 51, no. 1, Sept. 2018, pp. 878-888

[24]. *X. Xu, M. Ren, J. Cao, Q. Y. Wu, P. Y. Liu, and J. S. Lv*, "Spectroscopic diagnosis of zinc contaminated soils based on competitive adaptive reweighted sampling algorithm and an improved support vector machine", Spectroscopy Letters, vol.53, no. 2, Sept. 2020, pp. 86-99

[25]. *M. Dorigo, and L. M. Gambardella*, "Ant colony system: a cooperative learning approach to the traveling salesman problem", IEEE Trans on Ec, vol. 1, no. 1, Sept. 1997, pp. 53-66

[26]. *M. Mavrovouniotis, S. Yang, M. Van, C. Li, and M. Polycarpou*, "Ant Colony Optimization Algorithms for Dynamic Optimization: A Case Study of the Dynamic Travelling Salesperson Problem [Research Frontier]", IEEE Computational Intelligence Magazine, vol. 15, no. 1, Sept. 2020, pp. 52-63

[27]. *Y. Tan, J. Ouyang, Z. Zhang, Y. Lao, and P. Wen*, "Path planning for spot welding robots based on improved ant colony algorithm", Robotica, vol. 41, no. 3, Sept. 2023, pp. 926-938

[28]. *K. Y. Wang, G. Tarr, J. Y. Yang, and S. Mueller*, "Fast and approximate exhaustive variable selection for generalised linear models with APES", Australian & New Zealand Journal of Statistics, vol. 61, no. 4, Sept.2019, pp. 445–465

[29]. *J. Wang, W. Wang, Y. Hu, S. Tian, and D. Liu*, "Soil Moisture and Salinity Inversion Based on New Remote Sensing Index and Neural Network at a Salina-Alkaline Wetland", Water, 2021

[30]. *J. Holland*, Adaptation in Natural and Artificial Systems, University of Michigan Press, Ann Arbor, 1975.